Spin Density Maps in the Triplet Ground State of [Cu 2 (t -Bupy) 4 (N 3) 2](ClO 4) 2 (t -Bupy = p -tert -butylpyridine): A Polarized Neutron Diffraction Study

ARTICLE *in* JOURNAL OF THE AMERICAN CHEMICAL SOCIETY · JUNE 1998

Impact Factor: 12.11 · DOI: 10.1021/ja9739603

11 AUTHORS, INCLUDING:

Lars Öhrström
Chalmers University of Technology
131 PUBLICATIONS **1,801** CITATIONS

SEE PROFILE

Spin Density Maps in the Triplet Ground State of $[Cu_2(t\text{-Bupy})_4(N_3)_2](ClO_4)_2$ (*t*-Bupy = *p-tert*-butylpyridine): A Polarized Neutron Diffraction Study

Michael A. Aebersold,[†,‡] Béatrice Gillon,*[,†] Olivier Plantevin,[†] Luca Pardi,[†] Olivier Kahn,*[,‡,§] Pierre Bergerat,[§] Ingo von Seggern,[⊥] Felix Tuczek,[⊥] Lars Öhrström,[∥] André Grand,[∥] and E. Lelièvre-Berna[£]

Contribution from the Laboratoire Léon Brillouin, CEA-CNRS, Centre d'Etudes Nucléaires, Saclay, 91191 Gif sur Yvette, France, Laboratoire de Chimie Inorganique, URA CNRS no 420, Université de Paris Sud, 91405 Orsay, France, Laboratoire des Sciences Moléculaires, Institut de Chimie de la Matière Condensée de Bordeaux, UPR CNRS no 9048, 33608 Pessac, France, Institut für Anorganische und Analytische Chemie, Johannes Gutenberg Universität, D-55099 Mainz, Germany, Laboratoire de Chimie de Coordination, URA CNRS no 1194, Centre d'Etudes Nucléaires de Grenoble, 17 rue des Martyrs, 38041 Grenoble, France, and Institut Laue-Langevin, B.P. 156X, 38042 Grenoble, France

Received November 18, 1997

Abstract: This paper is devoted to the determination of the spin distribution in the spin triplet ground state of $[Cu_2(t\text{-Bupy})_4(N_3)_2](ClO_4)_2$, with *t*-Bupy = *p-tert*-butylpyridine. The crystal structure, previously solved at room temperature from X-ray diffraction, has been redetermined at 18 K from unpolarized neutron diffraction. The structure consists of binuclear cations in which Cu^{2+} ions are doubly bridged by azido groups in the 1,1-fashion, and noncoordinated perchlorate anions. The experimental spin distribution has been determined from polarized neutron diffraction (PND) at 1.6 K under 50 kOe. The spin populations have been found to be strongly positive on the Cu^{2+} ions, weakly positive on the terminal and bridging nitrogen atoms of the azido groups as well as on the nitrogen atoms of the *t*-Bupy ligands, and weakly negative on the central nitrogen atoms of the N_3^- bridges. The PND results have been discussed. The spin distribution in $[Cu_2(t\text{-Bupy})_4(N_3)_2](ClO_4)_2$ has been analyzed as resulting from a spin delocalization from the Cu^{2+} ions toward the azido bridges, to which a spin polarization effect within the azido π orbitals is superimposed. The experimental data have been compared to the results of DFT calculations. The spin density map is qualitatively reproduced; however, the DFT calculations overestimate the spin delocalization from the Cu^{2+} ions toward the peripheral and bridging ligands.

Introduction

The azido group, N_3^-, is certainly one of the most interesting magnetic couplers found so far in molecular magnetism. That is why so many azido-bridged polymetallic species have been synthesized and investigated in the last few years.[1−16] Two types of problems in particular have attracted the attention of the researchers. The former deals with the structural diversity of azido compounds. N_3^- can be both a terminal or a bridging ligand. When it is bridging, three kinds of structures can be encountered. N_3^- can bridge through the two terminal nitrogen atoms (μ-1,3-azido) either in a symmetrical or in a asymmetrical fashion. It can also bridge through only one of the terminal nitrogen atoms (μ-1,1-azido). The latter type of problems deals with the electronic versatility of azido-bridged species. In a first approximation the situation may be summed up as follows: N_3^- is a very efficient antiferromagnetic coupler when it bridges in the symmetrical 1,3-fashion, and a poor coupler when it bridges in the asymmetrical 1,3-fashion (which only

[†] Centre d'Etudes Nucléaires, Saclay.
[‡] Université de Paris Sud.
[§] Institut de Chimie de la Matière Condensée de Bordeaux.
[⊥] Johannes Gutenberg Universität.
[∥] Centre d'Etudes Nucléaires de Grenoble.
[£] Institut Laue-Langevin.

(1) Agnus, Y.; Louis, R.; Weiss, R. *J. Am. Chem. Soc.* **1979**, *101*, 3381.
(2) Kahn, O.; Sikorav, S.; Gouteron, J.; Jeannin, S.; Jeannin, Y. *Inorg. Chem.* **1983**, *22*, 2877.
(3) Sikorav, S.; Bkouche-Waksman, I.; Kahn, O. *Inorg. Chem.* **1984**, *23*, 490.
(4) Agnus, Y.; Louis, R.; Gisselbrecht, J.-P.; Weiss, R. *J. Am. Chem. Soc.* **1984**, *106*, 93.
(5) *Magneto-Structural Correlations in Exchange Coupled Systems*; Willet, R. D., Gatteschi, D., Kahn, O., Eds.; NATO ASI series, Reidel: Dordrecht, The Netherlands, 1985.
(6) Vicente, R.; Escuer, A.; Ribas, J.; El Fallah, M. S.; Solans, X.; Font-Bardia, M. *Inorg. Chem.* **1993**, *32*, 1920.
(7) Ribas, J.; Montfort, M.; Diaz, C.; Bastos, C.; Solans, X. *Inorg. Chem.* **1994**, *33*, 484.
(8) Ribas, J.; Monfort, M.; Ghosh, B. K.; Solans, X. *Angew. Chem., Int. Ed. Engl.* **1994**, *33*, 2087.
(9) Escuer, A.; Vicente, R.; Ribas, J. Solans, X. *Inorg. Chem.* **1995**, *34*, 1793.
(10) Beer, P. D.; Drew, M. G. B.; Leeson, P. B.; Lyssenko, K.; Ogden, M. I. *J. Chem. Soc., Chem. Commun.* **1995**, 929.
(11) Cortès, R.; Pizarro, L.; Arriotua, M. S.; Rojo, T. *Inorg. Chem.* **1994**, *33*, 2697.
(12) Escuer, A.; Vicente, R.; Goher, M. A. S.; Mautner, F. A. *Inorg. Chem.* **1996**, *35*, 6386.
(13) Montfort, M.; Ribas, J.; Solans, X.; Font-Bardia, M. *Inorg. Chem.* **1996**, *35*, 7633.
(14) Tandon, S. S.; Thompson, L. K.; Manuel, M. E.; Bridson, J. N. *Inorg. Chem.* **1994**, *33*, 5555.
(15) Thompson, L. K.; Tandon, S. S. *Comments Inorg. Chem.* **1996**, *18*, 125, and references therein.
(16) De Munno, G.; Poerio, T.; Viau, G.; Julve, M.; Lloret, F. *Angew. Chem., Int. Ed. Engl.* **1997**, *36*, 1459.

S0002-7863(97)03960-7 CCC: $15.00
Published on Web 05/15/1998

happens in Cu^{2+} chemistry). On the other hand, N_3^- is one of the very best ferromagnetic couplers when it bridges in the 1,1-fashion.[17,18] In all the structurally characterized compounds in which the metal ions are only bridged by 1,1-azido groups, the parallel spin state is the ground state, irrespective of the nature of these metal ions (provided obviously that they are magnetic).[2,3,6−11] When two metal ions are linked to each other by a 1,1-azido bridge together with another bridge, the situation may be more complicated. Most often, the overall coupling remains ferromagnetic. In a few cases the antiparallel spin state becomes the ground state.[14,15] Thompson was the first to suggest that such a situation could happen in Cu^{2+} chemistry when the Cu−N−Cu bridging angle on the azido side is larger than 108.5°. Subsequently, the same author realized that the effects of complementarity and countercomplementarity should be taken into account.[19,20] As a matter of fact, in polybridged species the overall coupling cannot be described as an algebraic sum of contributions arising from each of the bridges.[18] The electronic versatility of azido bridges also appears in one- or two-dimensional species in which the alternation of 1,1- and 1,3-coordinations leads to very interesting ferro- antiferromagnetic materials.[21,22]

The striking dichotomy between 1,1- and 1,3-azido bridges for many years has raised the question of the origin of this behavior. In particular, the mechanism of the ferromagnetic coupling through the 1,1-azido bridge has been addressed by several researchers.[15,17] To date, two interpretations have been proposed. The former is the simplest; it is based on a spin delocalization mechanism in the active-electron approximation. The stabilization of the parallel spin state would arise from an accidental orthogonality of the magnetic orbitals. If we restrict ourselves to di-μ-1,1-azido Cu^{2+} compounds, the situation would be very similar to that of di-μ-hydroxo Cu^{2+} compounds.[23] Only the value of the bridging angle for which there is a crossover between ferro- and antiferromagnetic couplings would be different. This value is around 97.5° for di-μ-hydroxo species[18,23] and is expected to be around 108° for di-μ-1,1-azido species.[15] The latter interpretation requires going beyond the active-electron approximation; it is based on a spin polarization mechanism, the basic ideas of which are recalled in the discussion section (spin distribution and ferromagnetic coupling subsection).[17] According to this interpretation, the coupling along the Cu^{2+}−1,1-N_3^-−Cu^{2+} linkage should be ferromagnetic, irrespective of the value of the Cu−N−Cu bridging angle. A third approach was also developed by one of us (F.T.) to interpret the spectroscopic properties of μ-1,1-azido Cu^{2+} binuclear species; it is based on a valence bond configuration interaction (VBCI) model.[24]

The physical data available so far essentially concern the relations between molecular structures and magnetic properties. Our opinion is that these data cannot tell us unambiguously which interpretation is the most appropriate. That is why we decided to determine the spin distribution in the triplet ground state of a μ-1,1-azido Cu^{2+} species. We selected the compound of formula $[Cu_2(t\text{-}Bupy)_4(N_3)_2](ClO_4)_2$, with *t*-Bupy = *p-tert*-butylpyridine, reported by one of us (O.K.) in 1983.[2] This compound has a spin triplet ground state, stabilized by more than 100 cm^{-1} with respect to the low-lying excited spin singlet state. Below ca. 100 K, only this ground triplet state is thermally populated. The EPR spectrum at 4.2 K is characteristic of a triplet state split in zero field.[25]

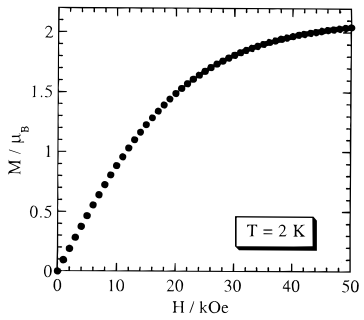

Figure 1. Field dependence of the magnetization at 2 K for $[Cu_2(t\text{-}Bupy)_4(N_3)_2](ClO_4)_2$.

The most informative description of the ground state of a magnetic molecular species is probably provided by the spin density maps. Such maps may be experimentally obtained from polarized neutron diffraction (PND) and theoretically calculated using quantum mechanical methods.[26−28] Here, both approaches will be used. More precisely, the paper is organized as follows: First, the nuclear structure of the compound is determined at 18 K by unpolarized neutron diffraction. Then, the spin density is reconstructed from the PND data at 1.6 K. Afterwards, the spin distribution is analyzed with respect to what the mechanisms recalled above would predict. Finally, the spin populations deduced from PND is compared to the results of a density functional theory (DFT) calculation. This provides new insights on the origin of the strong ferromagnetic coupling in μ-1,1-azido compounds.

Experimental Section and Calculation Methods

Synthesis. The synthesis of $[Cu_2(t\text{-}Bupy)_4(N_3)_2](ClO_4)_2$ was first described in ref 3. Large single crystals with a volume of about 10 mm^3 were obtained following a previously reported procedure.[24] The Neutron Laue technique was used to check the quality of the crystals and to orient them for the various experiments.

Magnetization. The field dependence of the magnetization was measured on a powder sample at 2 K with a Quantum Design SQUID magnetometer working up to 50 kOe. The results are shown in Figure 1 where the magnetization is expressed in Bohr Magnetons (μB). The magnetization under 50 kOe is equal to 2.05 μB, which is very close to the value expected for the saturation magnetization. Moreover, the magnetization versus field curve closely follows the Brillouin function for a triplet state.

Low Temperature Structure Determination through Neutron Diffraction. The room temperature crystal structure has already been determined by X-ray diffraction.[3] $[Cu_2(t\text{-}Bupy)_4(N_3)_2](ClO_4)_2$ crystallizes in the space group $P2_1/c$ with $Z = 2$. In order to analyze the polarized neutron data obtained at low temperature, it is necessary to

(17) Charlot, M.-F.; Kahn, O.; Chaillet, M.; Larrieu, C. *J. Am. Chem. Soc.* **1986**, *108*, 2574.
(18) Kahn, O. *Molecular Magnetism*; VCH: New York, 1993.
(19) Escuer, A.; Vicente, R.; Mautner, F. A.; Goher, M. A. S. *Inorg. Chem.* **1997**, *36*, 1233.
(20) Thompson, K. K.; Tandon, S. S.; Lloret, F.; Cano, J.; Julve, M. *Inorg. Chem.* **1997**, *36*, 3301.
(21) Cortès, R.; Drillon, M.; Solans, X.; Lezama L.; Rojo, T. *Inorg. Chem.* **1997**, *36*, 677.
(22) Escuer, A.; Vicente, R.; Goher, M. A. S.; Mautner, F. A. *Inorg. Chem.* **1997**, *36*, 3440.
(23) Crawford, W. H.; Richardson, H. W.; Wasson, J. R.; Hodgson, D. J.; Hatfield, W. E. *Inorg. Chem.* **1976**, *15*, 2107.
(24) von Seggern, I.; Tuczek, F.; Bensch, W. *Inorg. Chem.* **1995**, *34*, 5530.
(25) Boillot, M. L.; Journaux, Y.; Bencini, A.; Gatteschi, D.; Kahn, O. *Inorg. Chem.* **1985**, *24*, 263.
(26) Baron, V.; Gillon, B.; Plantevin, O.; Cousson, A.; Mathonière, C.; Kahn, O.; Grand, A.; Öhrström, L.; Delley B. *J. Am. Chem. Soc.* **1996**, *118*, 11822.
(27) Baron, V.; Gillon, b.; Cousson, A.; Mathonière, C.; Kahn, O.; Grand, A.; Öhrström, L.; Delley B.; Bonnet, M.; Boucherle J. X. *J. Am. Chem. Soc.* **1997**, *119*, 3500.
(28) Kahn, O.; Mathonière, C.; Srinivasan, B.; Gillon, B.; Baron, V.; Grand, A.; Öhrström L.; Ramasasha, S. *New. J. Chem.* **1997**, *21*, 1037.

Table 1. Crystallographic Data for the Structure Determination at 18 K

Crystallographic Data	
formula	$C_{26}H_{52}N_{10}O_8Cl_2Cu_2$
formula weight (g mol^{-1})	127.992
crystal system	monoclinic
space group	$P2_1/c$
color of crystal	dark blue
Z	2
density (g cm^{-3})	1.30
linear absorption coeff (cm^{-1})	1.69
Data Collection	
diffractometer	6T2 (Orphée)
monochromator	graphite
wavelength (Å)	1.51
crystal size (mm^3)	9
T (K)	18
no. of reflctns (cell refinement)	15
no. of measured reflcns	3209
no. of unique reflcns	1591
Conditions for Refinement and Agreement Factors[a]	
no. of unique reflcns N_O ($F > 3s$)	996
no. of refined params N_v	246
$R(F)$	0.063
$R_w(F)$	0.066
goodness of fit (GOF)	1.06

[a] $R(F) = (\sum_{hkl} ||F_o| - |F_c||)/(\sum_{hkl}|F_o|)$, $R_w(F) = [(\sum_{hkl} w(|F_o| - |F_c|)^2/(\sum_{hkl} w|F_o|^2)]^{1/2}$, and GOF $= [(\sum_{hkl} w(|F_o| - |F_c|)^2/(N_o - N_c)]^{1/2}$ with N_o = number of reflections, N_v = number of parameters, and w weighting scheme: $W = 1/\sigma^2$.

determine the atomic positions and the thermal parameters also at low temperature, particularly those of the hydrogen atoms. For this purpose an unpolarized neutron diffraction experiment was performed at 18 K on the four-circle spectrometer 6T2 at the Orphée reactor in Saclay, France. The information relative to the neutron data collection and structure refinement is summarized in Table 1. The crystal selected for this experiment had dimensions ($3 \times 2 \times 1.5$) mm^3 and was cooled down to 18 K in a Displex refrigerator. The cell parameters at 18 K were refined by least squares fitting of 15 reflections. At a wavelength of 1.51 Å, 1591 independent reflections were measured for $\sin(\theta/\lambda) < 0.54$ Å^{-1}. The integrated intensities were corrected by the Lorentz correction factor. No correction for absorption has been applied.

The least-squares refinement program CRYSTALS was used to determine the low temperature structure.[29] A set of 996 reflections with F_N^2 larger than 3σ was used to refine a total of 247 parameters. Two blocks of parameters were defined. The first block includes a scale factor and the thermal parameters, while the second block contains the atomic position parameters. All atoms were refined isotropically except the five hydrogen atoms having the largest anisotropic thermal parameters. An agreement factor $R_w(F_N) = 0.063$ was obtained using a weighting scheme $(1/\sigma)^2$. Extinction was not refined.

Polarized Neutron Diffraction Experiment. The polarized neutron diffraction is now a well established technique.[30] It is particularly useful to measure the small magnetic structure factors which can be induced by a strong applied field in paramagnetic systems containing a small number of unpaired electrons per molecule. The PND technique consists in measuring the flipping ratios $R(hkl)$ between the intensities diffracted by a single crystal for incident neutrons with polarization parallel (up) and antiparallel (down) to the applied field, respectively. In the case of centrosymmetrical crystal structures, these measurements yield the value of the ratio between the magnetic and nuclear structure factors. The experimental magnetic structure factors are then deduced from these data using the nuclear structure factors determined from unpolarized neutron diffraction measurements.

The information relative to the polarized neutron data collection is summarized in Table 2. The experiment was performed on the lifting counter diffractometer D3B at the ILL. The neutrons were monochromatized and polarized by a Heusler crystal, the wavelength of the incident neutrons being 0.843 Å and the beam polarization being 0.939(5). A magnetic field of 4.61 Tesla was applied vertically on the sample, and a flipper allowed for changing the polarization of the neutrons parallel and antiparallel to the applied field.

Table 2. Experimental Data Concerning the Polarized Neutron Measurements

Experimental Conditions	
diffractometer	D3(ILL)
monochromator	Heusler
wavelength (Å)	0.843
beam polarization	0.939(5)
flipping efficiency	1.000(1)
crystal size (mm^3)	9
vertical axis	c
T (K)	1.6
H (Tesla)	4.61
Data Collection	
no. of measured reflctns	549
no. of unique reflctns	253
no. of reflctns with $F_M > 3\sigma(F_M)$	152

The same crystal as for the structure determination was mounted with the c-axis parallel to the magnetic field. A restriction in the height of the lifting counter limited the observations to $0 < l < 5$. The data collection was restricted to the reflections for which the nuclear structure factor $|F_N|$ is larger than 2×10^{-12} cm, in order to avoid multiple scattering which may affect the weakest reflections. The flipping ratios were obtained by measuring the intensity on the Bragg peak and on the left and right background by rotating the crystal by ± 3 degrees. The data were collected at 1.6 K. The measurements included 549 reflections for $\sin(\theta/\lambda) < 0.32$ Å^{-1}. For most of the reflections two of the four equivalent reflections were measured. Equivalent Bragg reflections were combined, yielding 253 unique observations hkl, with $h = 0-7$, $k = 0-8$, and $l = 0-5$.

The magnetic structure factors were determined from the F_M/F_N ratios by calculating the nuclear structure factors from the low temperature structure (see above). A correction accounting for the nuclear polarization of the hydrogen atoms in the conditions of very low temperature and high magnetic field was applied to the experimental magnetic structure factors F_M^{exp}, taking a value of 15.9×10^{-3} μ_B for the hydrogen nuclear polarization.

The Cu^{2+} ion with the $3d^9$ configuration has an orbitally nondegenerate ground state. The contribution to the magnetization density arising from the interaction between the neutron magnetic moment and the magnetic field due to the orbital motion of the unpaired electron in principle should be taken into account. However, for most of the transition metal compounds the orbital moment is almost entirely quenched by the crystal field, and its effect can be treated as a correction. The orbital contribution was estimated, using the dipolar approximation for the orbital form factor[31]

$$f_{orb}(K) = [(g-2)/g](\langle j_0(K)\rangle + \langle j_2(K)\rangle) \quad (1)$$

in which g is the Cu^{2+} gyromagnetic ratio, K the length of the scattering vector, and $\langle j_l(K)\rangle$ the radial integral[32]

$$\langle j_l(K)\rangle = \int_0^\infty 4\pi r^2 R(r)^2 j_l(Kr)\, dr \quad (2)$$

where $R(r)$ is the 3d radial wavefunction for the Cu^{2+} unpaired electron and $j_l(Kr)$ the lth-order spherical Bessel function.

The average value of the g-factor was deduced from the EPR investigation[3,25] ($g_x = 2.07(2)$, $g_y = 2.03(2)$, $g_z = 2.24(2)$) using the

(29) Carruthers, J. R.; Watkin, D. J.; Betteridge, P. W. *CRYSTALS, an Advanced Crystallographic Program System*; University of Oxford: Oxford, England, 1988.

(30) Forsyth, J. B. *Atomic Energy Rev.* **1979**, *17*, 345.

(31) Brown, P. J. In *Magnetic Neutron Scattering and Magnetization Densities in Molecules and Crystals*; Becker, P., Ed.; NATO ASI Series, Plenum Press: 1980; p 268.

(32) Brown, P. J. *International Tables of Crystallography*; Cambridge University Press: 1992; p 391.

Table 3. Cell Parameters, Intramolecular Distances, Bond Lengths, and Angles at 298 and 18 K

	(T = 298 K)	(T = 18 K)
Cell Parameters (in Å)		
a (Å)	12.819(3)	12.716(13)
b (Å)	13.76(1)	13.441(13)
c (Å)	13.65(1)	13.094(13)
b (deg)	100.00(2)	99.282(1)
Intramolecular Distances (in Å)		
Cu−Cu′	3.042(3)	3.047(12)
N1−N1′	2.53(2)	2.552(9)
Bond Lengths (in Å) and Angles (in deg)		
Cu−N1	1.99(1)	1.989(7)
Cu′−N1	1.97(1)	1.985(7)
Cu−N4	2.00(1)	1.987(7)
Cu−N5	1.99(1)	1.984(7)
N1−N3	1.18(2)	1.187(7)
N2−N3	1.11(3)	1.148(7)
Cu−N1−Cu′	100.5(6)	100.1(3)
N1−Cu−N1′	79.5(5)	79.9(3)
Cu−N1−N2	130(3)	134.4(4)
Cu−N1′−N2′	123(3)	124.8(4)
N1−N2−N3	177(6)	179.4(6)

formula $g^2 = {}^1/_3(g_x^2+g_y^2+g_z^2)$, which yields $g = 2.115$. The $\langle j_0(K)\rangle$ and $\langle j_2(K)\rangle$ form factors for Cu^{2+} were taken from literature.[32]

The magnetic structure factors due to the orbital contribution were calculated from the expression

$$F_M^{orb}(K) = \sum_i m_i f_{orb}(K) \exp(-iKr_i) \quad (3)$$

where m_i is the induced magnetic moment per copper atom (assumed to be 1 μ_B).

The experimental spin contributions, F_M^{spin}, were then deduced by substraction of the orbital contributions from the experimental magnetic structure factors

$$F_M^{spin} = F_M^{exp} - F_m^{orb} \quad (4)$$

Density Functional Theory Calculations. The DFT calculations were performed using the DGauss DFT program[33] included in the UniChem package from Cray Research Inc.[34] The DZVP and TZ94P basis sets[35] were used, with the following compositions: DZVP: H [2s]; C, N [3s, 2p, 1d]; Cu [5s, 3p, 2d]. TZ94P: H [3s, 1p]; C, N [4s, 3p, 1d]; Cu [6s, 4p, 3d, 1f]. At the local spin density level the functional of Vosko, Wilk, and Nusair (VWN) was utilized.[36] For the nonlocal corrections to the exchange-correlation energy the Becke−Perdew (BP) functional[37] including a gradient corrected exchange was used in a perturbative way on the LSD-SCF. The spin density distribution was determined at the VWN level. The geometry used for the calculation was that of the actual compound, except that the *tert*-butyl groups were replaced by hydrogen atoms.

Description of the Nuclear Structure at 18 K

Table 3 displays the cell parameters, bond lengths, and angles at both room temperature and at 18 K. The atomic positions and thermal parameters at 18 K are given as Supporting Information. The corresponding molecular structure is represented in Figure 2. The molecular structure at room temperature has been previously described in details.[3] There are not significant changes in this structure with decreasing temperature. The N4 pyridine ring mean plane at 18 K is closely perpendicular to the bridging network CuN1N1′Cu′ with an angle of 89.7°, while the N5 pyridine ring forms an angle of 44.6° with the copper−azido plane.

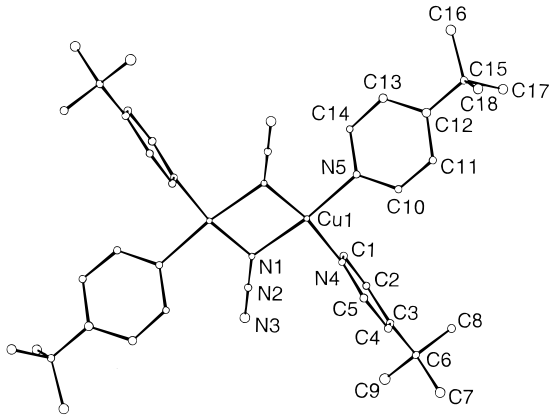

Figure 2. Molecular structure at 18 K of the binuclear cation [Cu$_2$(*t*-Bupy)$_4$(N$_3$)$_2$]$^{2+}$. Anisotropic thermal ellipsoïds are drawn when relevant.

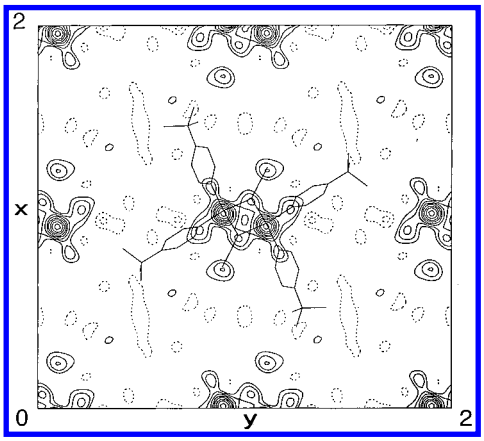

Figure 3. Spin density integrated along the c axis direction ($z = -0.25$ to 0.25). Four unit cells in the plane perpendicular to the c axis direction are represented ($x = 0-2$, $y = 0-2$). Levels are $\pm 0.01 \times 2^{n-1}$ μB Å^{-2}. Full and dashed lines represent positive and negative contours, respectively.

Spin Density Reconstruction

There are different possible approaches to analyze the experimental data of a PND experiment.[38] One of them is to extract the spin density in each point of the crystal cell directly from the measured structure factors F_M^{spin}. This Inverse Fourier method gives rather poor results because of the absence of structure factors not measured in the experiment.

A new method based on the maximum of entropy, MAXENT, permits us to reconstruct the spin density distribution without introducing any model.[39] This method evaluates the probability of each possible spin density map compatible with the limited set of data. The intrinsic probability of a map is expressed in term of entropy of the map. MAXENT then selects the most probable map which maximizes the entropy and keeps the agreement factor between calculated and observed magnetic

(33) Andzelm, J.; Wimmer, E. *J. Chem. Phys.* **1992**, *96*, 1280.
(34) UniChem 2.3; Cray Research, Inc. 2360 Pilot Knob Road, Mendota Heights, MN 55120, USA, 1994.
(35) Godbout, N.; Salahub, D. R.; Andzelm, J.; Wimmer, E. *Can. J. Chem.* **1992**, *70*, 560.
(36) Vosko, S. H.; Wilk, L.; Nusair, M. *Can. J. Phys.* **1980**, *58*, 1200.
(37) Becke, A. D. In *Density Functional Theories in Quantum Chemistry*: *Beyond the Local Density Approximation*; Becke, A. D., Ed.; ACS Symposium Series, Washington, D.C., 1989; Vol. 394, p 166 and references therein.
(38) Gillon, B.; Schweizer, J. In *Study of Chemical Bonding in Molecules: The interest of Polarized Neutron Diffraction. In Molecules in Physics, Chemistry and Biology*; Maruani, J., Ed.; Kluwer Academic Publisher: Dordrecht, The Netherlands, 1989; Vol. II, p 111.
(39) Papoular, R.; Gillon, B. *Europhys. Lett.* **1990**, *13*, 429.

Table 4. Model Refinements: Reliability Factors, Radial Coefficients, and Spin Populations P_{00} in μ_B[b]

	A	B
	spherical	p_x(N3) and d_{xy}(Cu) constraints
$R_w(F_M)$[a]	0.066	0.065
S	1.46	1.45
ζ_{Cu} (au^{-1})	9.0(3)	9.7(1)
ζ_N (au^{-1})	7(1)	7(2)
Cu	0.774(8)	0.783(7)
N1	0.069(7)	0.069(6)
N2	−0.015(6)	−0.016(6)
N3	0.054(7)	0.057(7)
N4	0.067(8)	0.067(8)
N5	0.048(7)	0.049(7)
C1	−0.034(8)	−0.036(8)
C2	0.009(9)	0.013(9)
C3	−0.013(10)	−0.014(11)
C4	0.015(9)	0.017(9)
C5	0.011(9)	0.009(9)
C10	0.010(9)	0.006(9)
C11	0.015(12)	0.014(13)
C12	−0.011(9)	−0.010(9)
C13	0.001(9)	0.000(9)
C14	−0.003(11)	−0.005(12)

[a] Same definition as in Table 1. [b] Normalized to $2\mu_B$ per molecule.

structure factors within error bars. The application of the maximum of entropy method to the set of 251 experimental magnetic structure factors (before correction for the orbital contribution) permits one to obtain the most probable spin density, in term of entropy, at each point of the cell. Figure 3 corresponds to the MAXENT spin density map integrated over the reduced coordinate z varying from −0.25 to 0.25 along the c axis direction. Only one half of the unit cell is represented for clarity. The other half can be directly deduced by symmetry operation. As expected, the spin density is mainly located on the copper atoms. Spin delocalization on the terminal nitrogen atoms N1 and N3 of the azido groups as well as on the nitrogen atoms N4 and N5 of the pyridine rings was clearly observed in this map. No spin density appeared on the carbon atoms.

The second possible data analysis consists in modeling the spin density distribution. A way to do so is the multipole modeling technique. The spin distribution depends on parameters which are determined as the best fit with the experimental data. For this analyzis a modification of the program MOLLY was used.[40,41] The spin density was described as a sum of atomic spin densities. The radial part of the atomic spin distributions was represented by a Slater-type function, the exponents of which were chosen from Hartree−Fock wave function calculations: $\zeta_{Cu} = 8.8$ au^{-1}, $\zeta_N = 3.9$ au^{-1}, $\zeta_C = 2.44$ au^{-1}.[42,43]

The experimental spin populations obtained after refinement are reported in Table 4. A set of 152 magnetic structure factors with $F_M > 3\sigma(F_M)$ was used in the refinements, with a weighting scheme $(1/\sigma)^2$. In a first model (A) spherical contributions were refined on all the non-hydrogen atoms except the carbon atoms of the *tert*-butyl groups. Only the copper and nitrogen radial exponents were refined. The populations reported in Table 4 are normalized to 2 μ_B per molecule. The sum of the populations before normalization was found equal to 1.92(6) μ_B.

(40) Hansen, N. K.; Coppens, P. *Acta Crystallogr.* **1978**, *A34*, 909.
(41) Ressouche, E. Ph.D. Thesis, Grenoble, 1994.
(42) Hehre, N. J.; Stewart, R. F.; Pople, J. A. *J. Chem. Phys.* **1969**, *51*, 2657.
(43) Clementi, E.; Raimondi, D. L. *J. Chem. Phys.* **1963**, *11*, 2686.

Table 5. Calculated Mulliken Spin Populations (μ_B) for the Model Compound $[Cu_2(py)_4(N_3)_2]^{2+}$ (py = pyridine)[a]

atom	DFT calculations	PND experiment
Cu	0.425	0.783(7)
N1	0.167	0.069(6)
N2	−0.005	−0.016(6)
N3	0.122	0.057(7)
N4	0.129	0.067(8)
N5	0.120	0.049(7)
C1	−0.002	−0.036(8)
C2	0.008	−0.013(9)
C3	−0.004	−0.014(11)
C4	0.008	0.017(9)
C5	−0.001	0.009(9)
C10	−0.002	0.006(9)
C11	0.006	0.014(13)
C12	−0.004	−0.010(9)
C13	0.008	0.000(9)
C14	0.000	−0.005(12)

[a] The results deduced from PND are reported for comparison.

In a second step, we attempted to apply different constraints to the spin density model and looked for their influence on the quality of the fit. On each nitrogen atom constraints of p_x, p_y, and p_z type were tested (the x axis is defined by the Cu−Cu′ direction, y is along the azido bonds, and z is perpendicular to the copper−azido plane). The only constraint which improved very slightly the agreement factor is a p_x-type density on the terminal atom N3 of the azido bridge. For the N4 and N5 atoms, p_σ constraints at least did not make the refinement worse, in contrast with a p_π constraint, which indicates that the N4 and N5 spin densities are more likely of the p_σ type. For the copper d_{xz}, d_{yz}, and d_{z^2} constraints clearly made worse the refinement ($R_w(F_M) = 0.07-0.08$), while d_{xy} and $d_{x^2-y^2}$ constraints did not modify the quality of the spherical refinement ($R_w(F_M) = 0.065$). It is not possible from the model refinement to discriminate between a d_{xy} and a $d_{x^2-y^2}$ distribution but the EPR data indicate that the Cu spin distribution is mainly of d_{xy} type. In the final model (refinement B) a d_{xy} type constraint for copper and a p_x type constraint for the terminal azido nitrogen atom N3 were applied.

The main features of the spin distribution obtained in the model refinement (B) are the following: (i) strong positive spin populations of 0.783(7) μ_B are found on each copper atom, (ii) positive spin populations are obtained on the terminal N1 and N3 nitrogen atoms of the azido groups (0.069(6) and 0.057(7) μ_B, respectively), and a small negative spin population is obtained on the central N2 atom (−0.016(6) μ_B), and (iii) a small dissymmetry appears in the spin delocalization toward the nitrogen atoms of the *t*-Bupy ligands; the spin population is greater on N4 (0.067(8) μB) than on N5 (0.049(7) μ_B). The spin populations on the carbon atoms of the terminal ligands are at the limit of the experimental accuracy but present the same trend; the spin delocalization toward one of the *t*-Bupy ligands is slightly more pronounced than toward the other one. The two pyridine rings differ by their dihedral angle with respect to the mean plane of the bridging network. The spin delocalization appears to be larger for the ring which is almost perpendicular to the copper−azido plane.

Figure 4 (parts a and b) shows the contours for the spin density integrated along a direction perpendicular to the (Cu−N1−Cu′) plane, for the spherical model (A) and the constrained model (B). These maps illustrate clearly the delocalization of the spin density from the Cu^{2+} ions toward the azido bridges and the nitrogen atoms of the *tert*-butylpyridine rings. They also emphasize the alternation of the spin densities along the azido groups.

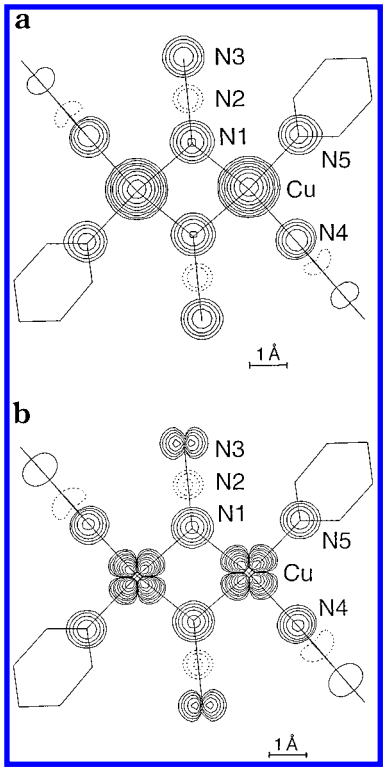

Figure 4. Spin density projection along a direction perpendicular to the Cu−N1−Cu′ plane obtained by multipole refinement: (a) for the spherical model (A) and (b) for the constrained model (B). The level contours are the same as in Figure 3.

Discussion

We will first analyze the mechanisms proposed to account for the ferromagnetic coupling through the 1,1-azido bridge in the light of the PND data, then we will see to what extend these data can be reproduced by DFT calculations. Finally, we will compare the spin distribution in the title compound to that reported for $[Cu_2(bipy)_4(OH)_2](SO_4)\cdot 4H_2O$.

Spin Distribution and Ferromagnetic Coupling. In the introduction we recalled that two mechanisms have been proposed to account for the ferromagnetic coupling through the 1,1-azido bridge. Let us now analyze what spin distribution each of these mechanisms would lead to. We begin by the spin delocalization mechanism. The two singly-occupied metal orbitals, d_A and d_B, along with the two highest doubly-occupied molecular orbitals (MOs) of N_3^-, of π_g symmetry, in the plane of the $Cu(N_3)_2Cu$ network are represented in Figure 5 (top). The mixing of these orbitals leads to the four molecular orbitals of Figure 5 (middle and bottom), where the symmetry labels refer to the irreducible representations of the D_{2d} symmetry group. At the active-electron approximation the wave function for the $M_S = 1$ component of the triplet state may be written as[18]

$$\Psi(S=1) = |b_{1g}\overline{b_{1g}}b_{3u}\overline{b_{3u}}b_{1g}{}^{*}b_{2u}| \qquad (5)$$

Such a wave function leads to large positive spin populations on the copper atoms and smaller positive spin populations on the bridging and terminal nitrogen atoms of N_3^-. The spin population on the central nitrogen atom of N_3^- is expected to be negligibly small. Such a spin distribution is in line with what has been found, except as far as the central nitrogen atom is concerned. Let us point out that no negative spin population can be found at this level of approximation.

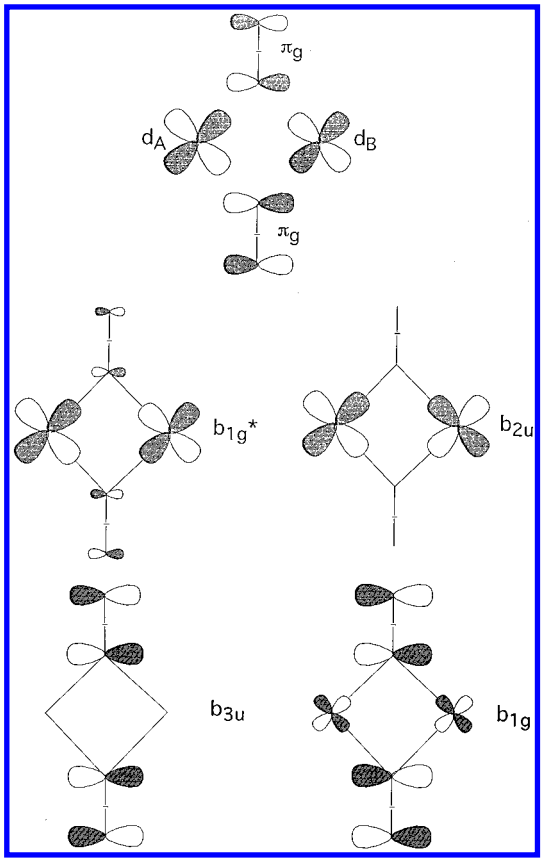

Figure 5. Top: d metal orbitals and π_g azido orbitals in the plane of the bridging network. Middle: singly-occupied molecular orbitals in the ground triplet state. Bottom: Doubly-occupied orbitals of highest energy in the ground triplet state.

Let us now consider the spin polarization mechanism. Within each π_g orbital of N_3^- the two electron spins would be polarized in such a way that the spin populations would be positive at an extremity, say on the terminal nitrogen atom, and negative at the other extremity, say on the bridging nitrogen atom. The delocalization of the β spin from the bridging nitrogen toward the d_A and d_B metal orbitals would stabilize the state in which the two metal electrons have the α spin, as a consequence of Hund's rule. Therefore, this mechanism leads to large positive spin populations on the copper atoms, smaller positive spin populations on the terminal nitrogen atoms, and small negative spin populations on the bridging nitrogen atoms. One immediately sees that these predictions are not in line with the experimental findings. At this stage it clearly appears that the spin delocalization model is more appropriate than the spin polarization model. However, it is necessary to go beyond the active-electron approximation to understand why significant negative spin populations are found on the central nitrogen atoms. So far, the lowest unoccupied molecular orbitals of N_3^-, of π_u symmetry, were ignored. One of them is represented in Figure 6 (top). The two π_u orbitals in the idealized D_{2h} symmetry of the complex give the $b_{1g}{}^*$ and b_{3u} molecular orbitals represented in Figure 6 (bottom). The wavefunctions for the $M_S = 1$ components of the two excited triplet states may be written as

$$\Psi_1{}^{e}(S=1) = |b_{1g}\overline{b_{1g}}{}^{e}b_{3u}\overline{b_{3u}}b_{1g}{}^{*}b_{2u}|$$

$$\Psi_2{}^{e}(S=1) = |b_{1g}\overline{b_{1g}}b_{3u}\overline{b_{3u}}{}^{e}b_{1g}{}^{*}b_{2u}| \qquad (6)$$

These excited states have the same symmetry as the ground

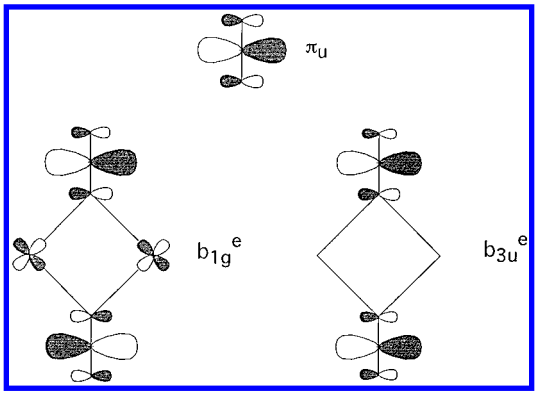

Figure 6. Top: π_u azido orbital. Bottom: unoccupied molecular orbitals resulting from the mixing of the π_u azido orbitals with the d metal orbitals.

triplet state. The configuration interaction between these three triplet states brings some negative spin population on the central nitrogen atoms, according to a spin polarization mechanism which has been well documented in the case of the allyl radical.[18,44] It is interesting to note here that the importance of the azido π_u orbital in modulating the magnitude of the coupling was recognized in the VBCI model.[24]

All together, the spin distribution in $[Cu_2(t\text{-Bupy})_4(N_3)_2](ClO_4)_2$ may be understood as resulting from two mechanisms: first a spin delocalization from the Cu^{2+} ions toward the azido bridges and then a spin polarization within the π orbitals of the azido groups.

Of course, the discussion above is oversimplified, and we intend to come back to the theory of the interaction through the azido bridge in a subsequent paper. A few points, however, may already be stressed here. In the delocalization mechanism only the in-plane highest-occupied MO of N_3^-, $1\pi_g$, was considered. The $3\sigma_u$ and $4\sigma_g$ orbitals just below in energy certainly play an important role. Concerning the spin polarization mechanism, what was refuted above is the initial and simple picture of this mechanism leading to a negative spin population on the bridging nitrogen atom of N_3^-. On the other hand, the spin Hamiltonian formalism developed in ref 17 might remain valid. We will also explore this in our forthcoming theoretical paper.

DFT Calculations. The spin populations in the triplet state obtained by DFT calculations using a Mulliken population analysis[45] are given in Table 5. A representation of the spin density is shown in Figure 7.

Most of the spin density is localized on the copper atoms. A delocalization toward the terminal nitrogen atoms of the azido groups as well as the nitrogen atoms of the *t*-Bupy rings is found. As for the other compounds containing Cu^{2+} ions studied by both PND and DFT methods, the calculated spin delocalization from the metal ion toward the first nearest neighbors is overestimated with respect to the PND results.[26−28] However, the main features of the calculated spin density agree well with the experimental data. Positive spin populations are found on the N1 and N3 nitrogen atoms of the azido bridge, with a larger population on N1 than on N3. In addition, a small negative spin population is found on the central nitrogen atom N2. The spin population on the N4 atom of the *t*-Bupy ring appears to be slightly larger than on N5. The calculation yields alternate positive and negative spin populations on the rings.

(44) Salem, L. *The Molecular Orbital Theory of Conjugated Systems*; Benjamin: New York, 1966.
(45) Mulliken, R. S. *J. Chem. Phys.* **1955**, *23*, 1833.

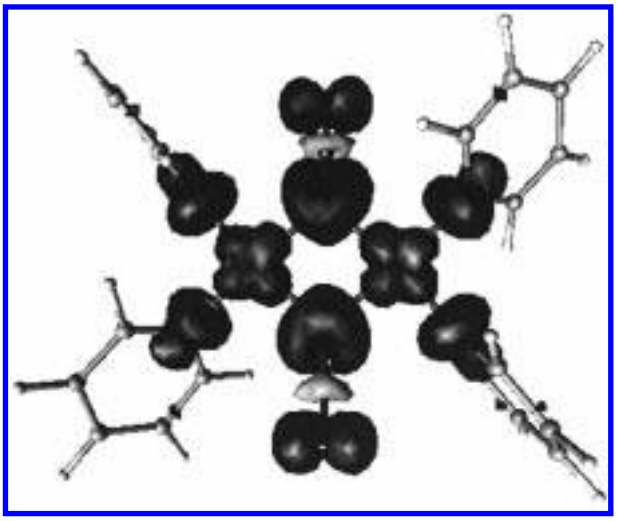

Figure 7. Representation of the spin density in $[Cu_2(t\text{-Bupy})_4(N_3)_2](ClO_4)_2$ obtained from DFT calculations. The minimal positive and negative level is $\pm 10^{-3}$ e/A^3.

Comparison between $[Cu_2(t\text{-Bupy})_4(N_3)_4](ClO_4)_2$ and $[Cu_2(bipy)_4(OH)_2](ClO_4)_2$. In 1983 Figgis and co-workers reported on the spin distribution for another Cu^{2+} binuclear compound with a triplet ground state, $[Cu_2(bipy)_4(OH)_2](SO_4)\cdot 4H_2O$.[46] We would like to compare briefly the two sets of data. For $[Cu_2(bipy)_4(OH)_2](SO_4)\cdot 4H_2O$ the spin populations were found to be positive on the copper (0.85 μ_B), bridging oxygen (0.10 μ_B), and terminal nitrogen (0.05 μ_B) atoms. The spin delocalization is therefore slightly less pronounced than in the title compound. In other respects, zones of negative spin density were found around the bridging oxygen atoms, directed so as to bisect the bonds of the copper atoms, but on the reverse side of the atom. These negative spin densities emphasize again the duality between spin delocalization and spin polarization in magnetic molecular compounds.

Conclusion

Two decades ago or so, some chemists did not believe that the interaction within a binuclear compound could be ferromagnetic. When the first paper dealing with the title compound was submitted, one of the reviewers claimed that the results were certainly erroneous because the ground state of a Cu^{2+} pair could not be the triplet state! Now, it is well established that the occurrence of ferromagnetic interaction is far from being exceptional, even if the factors governing the stabilization of the parallel spin state are not all perfectly understood yet. In particular, it has been unambiguously demonstrated that the 1,1-azido bridge has a remarkable capability to couple ferromagnetically magnetic centers.

This work reveals that the spin distribution in the triplet ground state of $[Cu_2(t\text{-Bupy})_4(N_3)_4](ClO_4)_2$ is dominated by a spin delocalization mechanism, to which is superimposed a spin polarization effect within the π orbitals of the azido groups. Probably, the two singly-occupied orbitals in the triplet state, b_{2u} and b_{1g}*, are very close in energy, so that the ferromagnetic component governed by the two-electron exchange integral between the magnetic orbitals dominates.[18] If this work brings

(46) Figgis, B. N.; Mason, R.; Smith, A. R. P.; Varghese, J. N.; Williams, G. A. *J. Chem. Soc., Dalton Trans.* **1983**, 703.

important insights on the coupling through the $Cu^{2+}-1,1\text{-}N_3^{-}-Cu^{2+}$ linkage, it leaves at least one open question. Is the nature of the coupling in such μ-1,1-azido species as sensitive to small variations of the bridging angle as in μ-hydroxo species? In other words, can the 1,1-azido group be considered as an almost universal ferromagnetic coupler, or is the stabilization of the parallel spin state only achieved in a limited range of bridging angle values? We hope to be able to answer this question in the rather near future.

Acknowledgment. We thank A. Gukasov, responsible for the four-circle neutron diffractometer at the LLB for his help in the low temperature structure determination.

Supporting Information Available: Tables of detailed structure determination, reduced coordinates, and thermal parameters (3 pages print/PDF). See any current masthead page for ordering and Web access instructions.

JA9739603